Annals of Botany **90**: 765–773, 2002
doi:10.1093/aob/mcf258, available online at www.aob.oupjournals.org

Structural Basis of the Rind Disorder Oleocellosis in Washington Navel Orange (*Citrus sinensis* L. Osbeck)

TOBY G. KNIGHT, ANDREAS KLIEBER and MARGARET SEDGLEY*

Department of Horticulture, Viticulture and Oenology, Waite Campus, The University of Adelaide, Glen Osmond, South Australia 5064, Australia

Received: 1 July 2002 Returned for revision: 7 August 2002 Accepted: 18 September 2002 Published electronically: 24 October 2002

Oleocellosis, a physiological rind disorder of citrus fruit, is an unattractive surface blemish caused by phytotoxic effects of released rind oils. The development of oleocellosis in Washington navel orange (*Citrus sinensis* L. Osbeck) was examined by following a time sequence of surface symptoms and microscopic rind changes. The two natural causes of oleocellosis were simulated: mechanical damage to the fruit and transfer of rind oil between fruit. Mechanical fruit injury resulted in rupture of the epidermis above oil glands. Released surface oil appeared to infiltrate the rind via the ruptured epidermis resulting in rapid degeneration of cortical, but not epidermal, cell contents. Oil application to the rind surface produced a more severe blemish than did mechanical damage. The oil appeared to diffuse through the cuticle causing degeneration of the contents of all cell layers, including the epidermis. Loss of membrane integrity was detected within 30 min, followed by cell content degeneration and cell collapse. The resulting blemish, characterized by rind collapse and darkening, developed substantially within 3 d and was attributed to the cellular damage.

Key words: Oleocellosis, rind disorder, rind oil, Washington navel orange, *Citrus sinensis* L. Osbeck, light microscopy, electron microscopy, confocal microscopy.

INTRODUCTION

Oleocellosis is a physiological rind disorder of citrus fruit that is caused by the action of phytotoxic rind oils on the rind tissue. These oils are released from glands located in the rind (Knight *et al*., 2001) following mechanical damage to the fruit (Fawcett, 1916). Oleocellosis can result from various types of damage, including insect attack, hail damage or wind rub (Whiteside *et al*., 1988), and can also develop in undamaged fruit that come into contact with damaged fruit. The oleocellosis-damaged rind has a sunken and discoloured appearance (Shomer and Erner, 1989) and, in immature fruit, fails to colour normally, leaving a green/yellow area (Fawcett, 1916).

The mechanism underlying oleocellosis development is not clearly understood. Mechanical fruit damage has been observed to result in surface oil release (Fawcett, 1916; Cahoon *et al*., 1964; Eaks, 1968), and epidermal rupture above glands has been observed in damaged fruit using light microscopy (LM) (Labuschagne *et al*., 1977; du Plessis, 1978). However, it has also been suggested that oil may be released directly into the rind tissue, based on the presence of sub-surface rind damage between glands in oleocellosis-affected tissue (du Plessis, 1978; Shomer and Erner, 1989) and the development of symptoms in fruit despite the removal of surface oil (Loveys *et al*., 1998).

The nature of the reaction between the phytotoxic oils and the rind tissue is also ill-defined in the literature. In the most detailed studies to date, oleocellosis has been examined in de-greened Shamouti orange fruit (Shomer and Erner, 1989) and mature Valencia orange fruit (B. L. Wild, pers. comm.). These studies show discrepancies based on LM and transmission electron microscope (TEM) observations. Using LM, Shomer and Erner (1989) reported oleocellosis rind damage to occur either sub-epidermally or in all rind layers, whereas Wild (pers. comm.) observed densely aggregated upper rind layers only. Using TEM, Shomer and Erner (1989) described a process of cell plasmolysis and collapse, and attributed the green colour of damaged tissue to the presence of 'giant chloroplasts'. Wild (pers. comm.) attributed flattened cell layers to abnormal cell division rather than cell collapse.

In this paper, oleocellosis development is examined in mature Washington navel orange fruit by following a time sequence of surface symptoms and microscopic changes in the rind, observed using LM and TEM. Scanning electron microscopy (SEM) and confocal microscopy were also employed. The two natural causes of oleocellosis were simulated in the laboratory.

MATERIALS AND METHODS

Plant material

Mature fruit were collected from four 40-year-old Washington navel orange trees in an orchard located at Mypolonga, South Australia. Fruit sampling was based on uniformity of fruit size and fruit colour, as fruit colour has been reported to influence oleocellosis blemish perception (Levy *et al*., 1979; Erner, 1982).

* For correspondence. Fax +61 8 8303 7116, e-mail margaret.sedgley@adelaide.edu.au

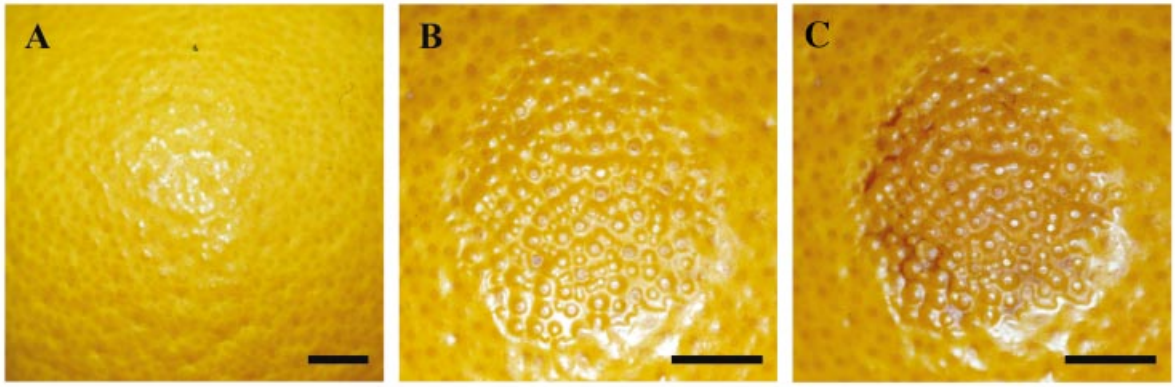

FIG. 1. Blemish severity scoring for oleocellosis symptoms. A, No collapse and no discolouration (0, 0) in untreated tissue. B, Slight collapse and very slight discolouration (2, 1), 48 h after oil application. C, High collapse and extreme discolouration (4, 5), 10 d after oil application. Surface protuberances indicate the location of oil glands. Bars = 1 cm.

Fruit were picked from the eastern aspect of the tree, as these fruit normally show higher turgor, indicating greater susceptibility to mechanical oil gland rupture (Loveys *et al*., 1998). Fruit were picked at 0900 h to avoid the decline in turgor due to increasing temperature and decreasing relative humidity throughout the day (Cahoon *et al*., 1964). Fruit were handled with care and, after harvest, were individually wrapped in wet paper towels to retain water. They were pattern-packed into plastic-lined crates, with cushioning between fruit layers.

Oleocellosis induction

Oleocellosis was induced approx. 1 h after harvest using two methods: penetrometer damage and surface oil application. The penetrometer is used commercially to measure 'rind oil release pressure (RORP)', which is used to predict oleocellosis occurrence prior to harvest (Cahoon *et al*., 1964). A penetrometer with an 8-mm diameter transparent acrylic tip was used. Compared with brass-tipped penetrometers used in previous studies (Cahoon *et al*., 1964; Eaks, 1968; Shomer and Erner, 1989), the use of an acrylic-tipped penetrometer has been shown to provide more accurate RORP readings (Loveys *et al*., 1998). Standard damage was achieved by applying RORP to each fruit. To apply oils, a method similar to that of Wild (1998) was used: 15 µl of d-limonene, the major component of orange oil (Shaw, 1979), was pipetted onto 6-mm cardboard discs (Antibiotic Assay discs; Whatman International Ltd, Maidstone, UK), which were attached to the fruit surface using adhesive tape. Non-phytotoxic sunflower oil was included as a control oil treatment. Each induction method was replicated twice on each fruit.

Symptom assessment

Following induction, symptoms were assessed at eight time-intervals over 3 d: 30 min and 1, 2, 6, 12, 24, 48 and 72 h. Observations were also made after 10 d.

Blemish severity was assessed using a scoring system. Rind collapse and discolouration were assessed using two separate subjective scales. For collapse the scale was: 0 (nil), 1 (very slight), 2 (slight), 3 (medium) and 4 (high). Discolouration was scored as: 0 (nil), 1 (very slight), 2 (slight), 3 (medium), 4 (high) and 5 (extreme). Figure 1 shows three blemish images, with their severity scores. A single observer scored blemishes.

Experimental design

In expt 1, 15 mature fruit were collected from one tree, and all fruit were assessed at each time interval for symptom development. In expt 2, 72 fruit were harvested from three trees and fruit were destructively sampled for microscopy. Nine fruit (three trees × three replicates) were allocated to each time interval.

Statistical analysis

Rind collapse and discolouration data were analysed using the statistical package Genstat for Windows version 5.41 (Lawes Agricultural Trust, IACR Rothamsted, UK). A split-plot design was applied to the data, and ANOVA tables were used to test for statistical significance at the 95 % confidence level.

Sampling for microscopy

At each time interval, samples were collected for LM and TEM preparation. For both penetrometer- and oil-induced oleocellosis, samples were taken from the application site, the area directly adjacent to the application site and an untreated (control) area.

Light microscopy (LM)

Rind samples 5 × 5 mm were fixed overnight in 3 % glutaraldehyde in 0·025 M phosphate buffer, dehydrated

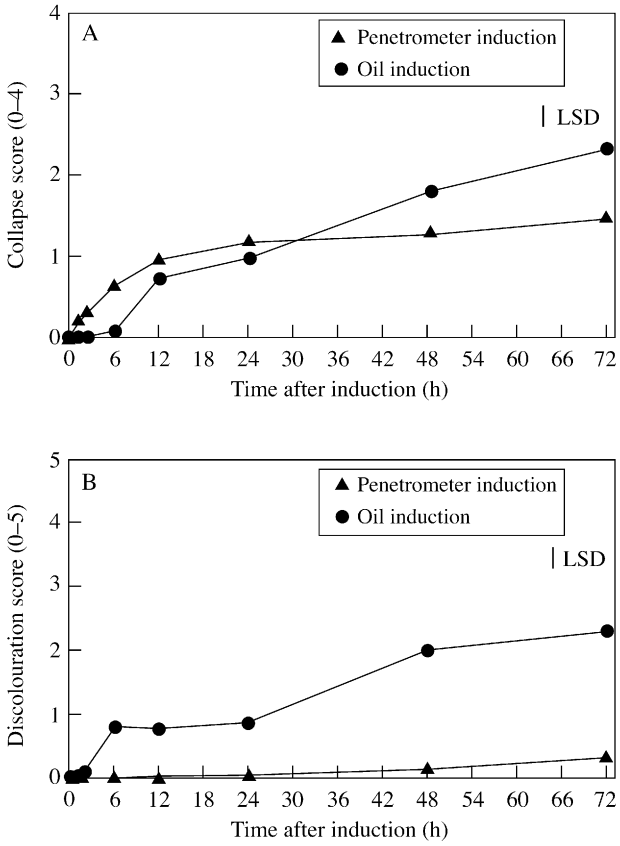

FIG. 2. Relationship between time and rind collapse (A) and discolouration (B). Collapse score: 0 (nil), 1 (very slight), 2 (slight), 3 (medium) and 4 (high). Discolouration score: 0 (nil), 1 (very slight), 2 (slight), 3 (medium), 4 (high) and 5 (extreme). LSD = 0·26 (A) and 0·33 (B).

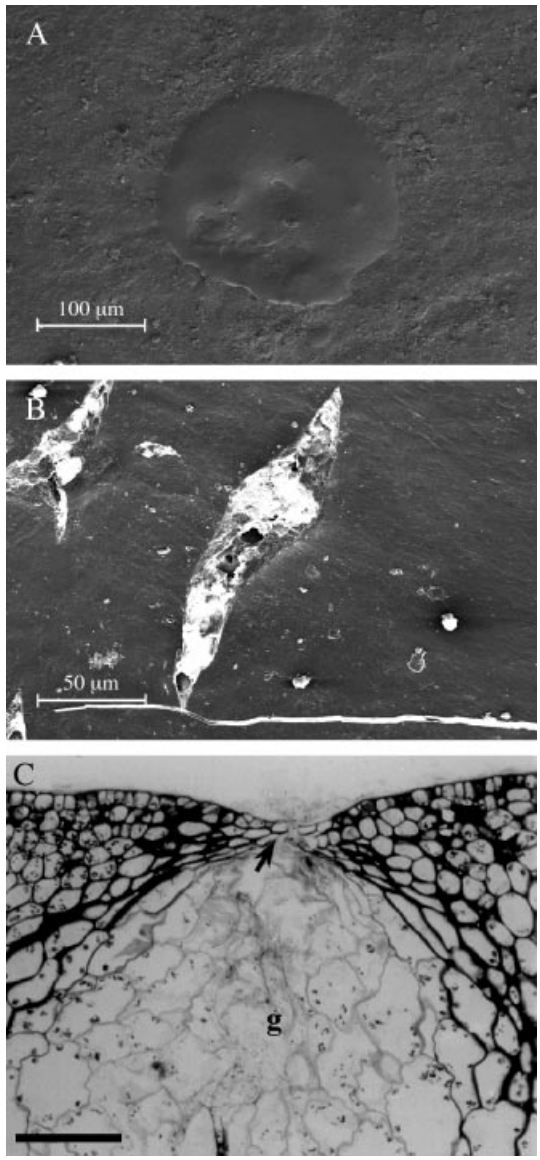

FIG. 3. Rind surface damage due to penetrometer action. A, SEM image of oil pool on the rind surface above a ruptured gland, immediately after damage. Bar = 100 µm. B, SEM image of tears and cracks in the rind surface, immediately after damage. Bar = 50 µm. C, Longitudinal, aldehyde-fixed, PAS/TBO stained section of the ruptured epidermis (arrow) above a gland (g), immediately after damage. Bar = 100 µm.

through an alcohol series and embedded in glycol-methacrylate (Knight *et al*., 2001). Sections (4 µm thick) were stained with periodic acid Schiff's reagent (PAS) and Toluidine Blue O (TBO) (O'Brien and McCully, 1981).

Histochemical staining for lignin using Phloroglucinol-HCl (Jensen, 1962) and suberin using Sudan Black B (O'Brien and McCully, 1981) was also employed. All material was observed under a Zeiss Axiophot Photo-microscope, using transmitted light.

Transmission electron microscopy (TEM)

Rind samples 1 × 1 mm were fixed overnight in 4 % paraformaldehyde/1·25 % glutaraldehyde plus 4 % sucrose buffered to pH 7·2 in phosphate-buffered saline, post-fixed in phosphate-buffered 1 % osmium tetroxide, dehydrated through an acetone series and embedded in Procure-Araldite resin (Knight *et al*., 2001). Ultra-thin sections were collected on collodion-coated copper grids, stained with uranyl acetate and lead citrate (O'Brien and McCully, 1981) and viewed using a Philips CM 100 TEM. Montage images of the rind profile were created with analySIS (Soft Imaging Systems, Münster, Germany). The ultrastructural integrity of epidermal (outer), hypodermal (second and third) and cortex (underlying) layers were examined separately.

Scanning electron microscopy (SEM)

Healthy and oleocellosis-damaged rind samples of approx. 2 × 3 mm were mounted onto aluminium stubs using carbon paint. Samples were plunge frozen in liquid nitrogen slush, and transferred under vacuum to the prechamber of an Oxford CT 1500 HF cryotransfer system, maintained at approx. –130 °C. Samples were sublimed for approx. 3 min at –92 °C and 5 × 10^{-5} Pa, re-cooled to –110 °C, and coated with gold palladium. Samples were

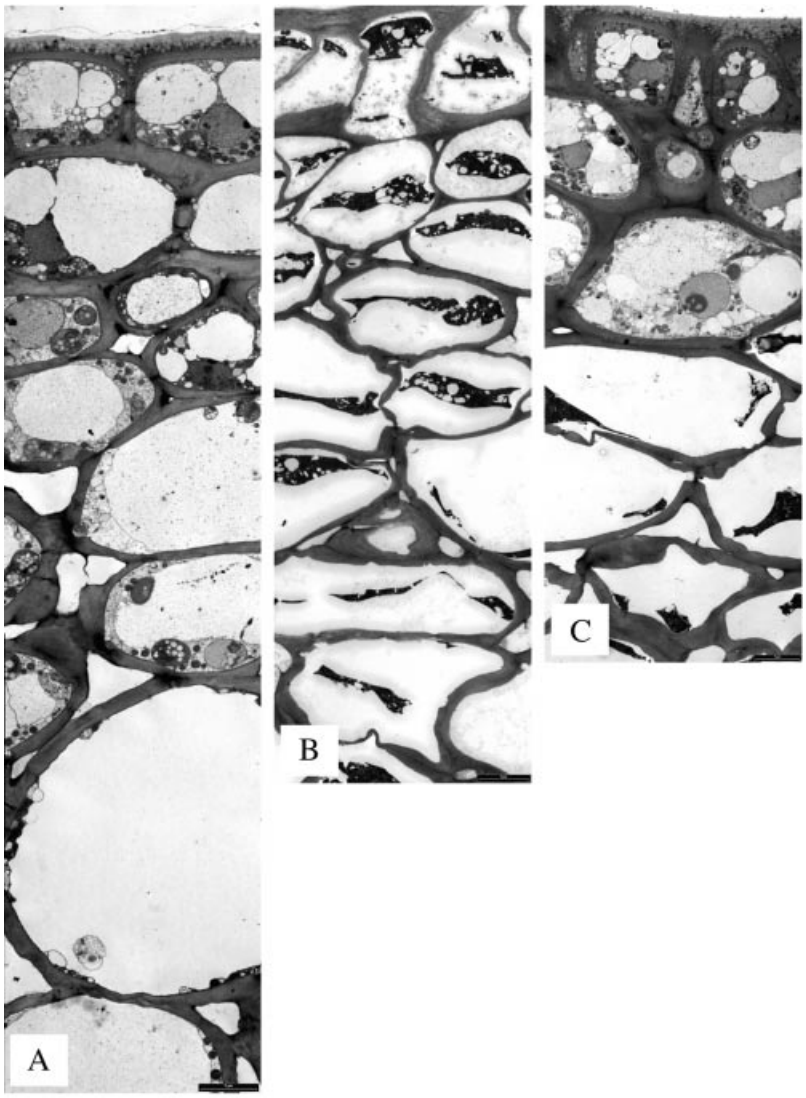

FIG. 4. Rind sub-surface damage, profile images. A, Untreated (control) tissue. B, Oil-treated tissue after 2 d, medium level blemish (collapse = 3, discolouration = 4). C, Penetrometer-damaged tissue after 3 d, medium level blemish (collapse = 3, discolouration = 2). Bars = 5 μm.

transferred to the cold stage of the Philips XL 30 FEGSEM, and examined at approx. –190 °C.

Confocal microscopy

Tissue sections approx. 2 mm thick and 15 mm long were collected from healthy and oleocellosis-damaged tissue. Sections were stained with 0·01 % Nile Red (Sigma, St Louis, MO, USA) (Brundrett *et al*., 1991), rinsed and counterstained with 0·01 % Calcofluor White M2R (Sigma) (Hughes and McCully, 1975). Sections were mounted in 75 % glycerol and examined using a Bio-Rad Radiance 2000 MP visualizing system attached to a Nikon Eclipse TE300 inverted microscope. A Coherent Mira900-F titanium : sapphire ultrafast laser was used to excite the specimen at 770 nm, and images were collected using emission filters 620/100 nm (for Nile Red) and 450/80 nm (for Calcofluor White).

RESULTS

Symptoms

The period of most rapid collapse for penetrometer-damaged fruit was within the first 12 h, with significant increases ($P < 0·05$) observed between 2 and 6 h, and again between 6 and 12 h (Fig. 2A). Oil-treated fruit also showed a significant increase in damage between 6 and 12 h, and also at later stages, between 24 and 48, and 48 and 72 h. By day 3, mean collapse scores were 2·3 for oil-treated fruit and 1·5 for penetrometer-damaged fruit. Oil-treated fruit showed a mean discolouration score of 2·3, compared with the

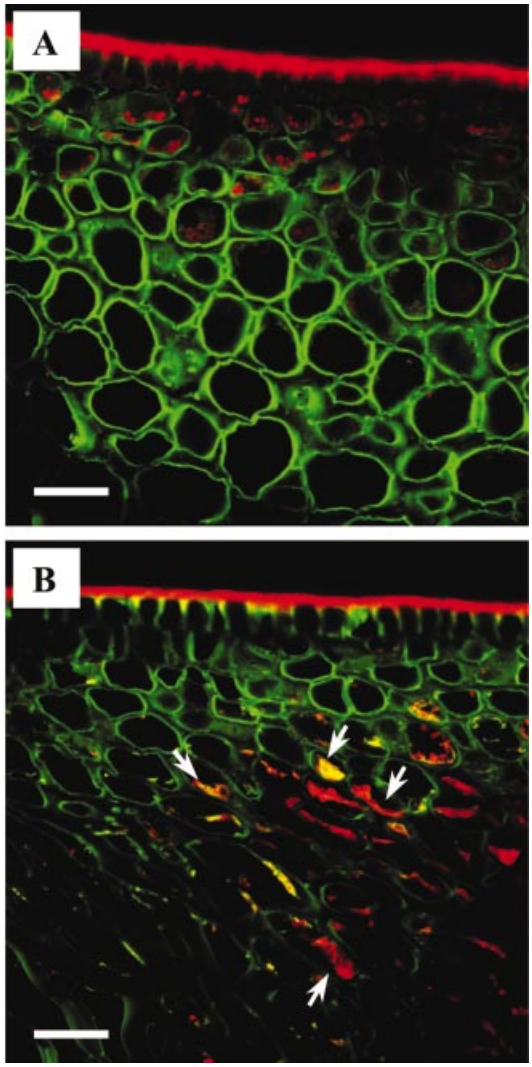

FIG. 5. Rind oil localization using confocal microscopy. Two-colour merged optical sections of fresh tissue, stained with Calcofluor White for cell walls (green) and Nile Red for lipid (red). Tissue regions between oil glands depicted. A, Untreated (control) tissue. B, Penetrometer-damaged tissue after 3 d, showing degenerated contents of cells and lipid (arrows) stained by Nile Red. Bars = 30 μm.

maximum score of 0·3 at day 3 for penetrometer-damaged fruit (Fig. 2B). In oil-treated fruit, a significant increase in darkening ($P < 0·05$) was observed between 2 and 6 h, and 24 and 48 h. The non-phytotoxic sunflower oil did not produce symptoms.

Surface damage

Following penetrometer damage, a pool of oil was visible above each ruptured gland (Fig. 3A). At the edge of the zone of penetrometer application, surface cracks and tears were also present (Fig. 3B). Epidermal rupture above glands was detected in LM sections (Fig. 3C). None of these features was apparent on the surface of untreated tissue. Surface cracks and tears were not observed following oil application.

Sub-surface damage

Oil-damaged cells showed degeneration and collapse, which were not observed in untreated tissue (Fig. 4A). A difference in the localization of sub-surface damage was observed between penetrometer-damaged and oil-treated fruit. In oil-treated fruit, cells with degenerated contents were located in all cell layers from the epidermis downwards (Fig. 4B). However, in penetrometer-damaged tissue, the majority of samples showed cells with degenerated contents localized to the cortex layers, below intact epidermal and hypodermal layers (Fig. 4C). The cell wall between hypodermal (intact) and cortex (damaged) cells appeared to be structurally sound, and plasmodesmata were observed between these cell layers. Histochemical staining showed lignin and suberin to be absent in both untreated and oleocellosis-damaged tissue.

Rind oil localization

Using confocal microscopy, untreated rind tissue showed small, fluorescent lipid bodies in the upper rind layers which were plastoglobuli in plastids or cytoplasm-localized oil bodies. Three days after penetrometer damage, the degenerated contents of oil-damaged cells observed in fixed tissue with TEM were also detected in fresh tissue (Fig. 5B). Degenerated cell contents were stained by the lipid stain Nile Red.

Oleocellosis development

Major structural changes were observed in the overall profile of the rind (Fig. 6), and in the ultrastructural details of the cells (Fig. 7).

Untreated tissue prepared for TEM was well preserved, with all cell layers showing intact organelles and membrane systems (Fig. 4A). Nuclei showed an intact nuclear envelope, often with very slight expansion of the perinuclear space (Fig. 7A). Plastids, in the form of chromoplasts, were usually round to oval-shaped and showed an intact outer membrane, folded inner membrane and lightly stained plastoglobuli (Fig. 7B). Mitochondria showed an intact double membrane, with internal cristae (Fig. 7C). Round to oval-shaped oil bodies were observed in the vacuole and cytoplasm, and oil movement between the two compartments was observed.

Thirty minutes after oil treatment, external symptoms had not developed and the rind profile (Fig. 6A) appeared similar to that of untreated tissue. Nevertheless, ultrastructural degeneration was already apparent. In epidermal and hypodermal layers, the tonoplast and plasmalemma of some cells were discontinuous. Nuclei showed slight to significant expansion of the perinuclear space (Fig. 7D), and plastids showed signs of membrane degeneration (Fig. 7E). Some cortex cells appeared intact, whilst in others the cytoplasm showed a granular appearance and few mitochondria were detected. Oil bodies were larger and more numerous than in untreated tissue, and were present in the vacuole and cytoplasm. Oil bodies appeared to be more closely associated with organelles, for example, mitochondria (Fig. 7F).

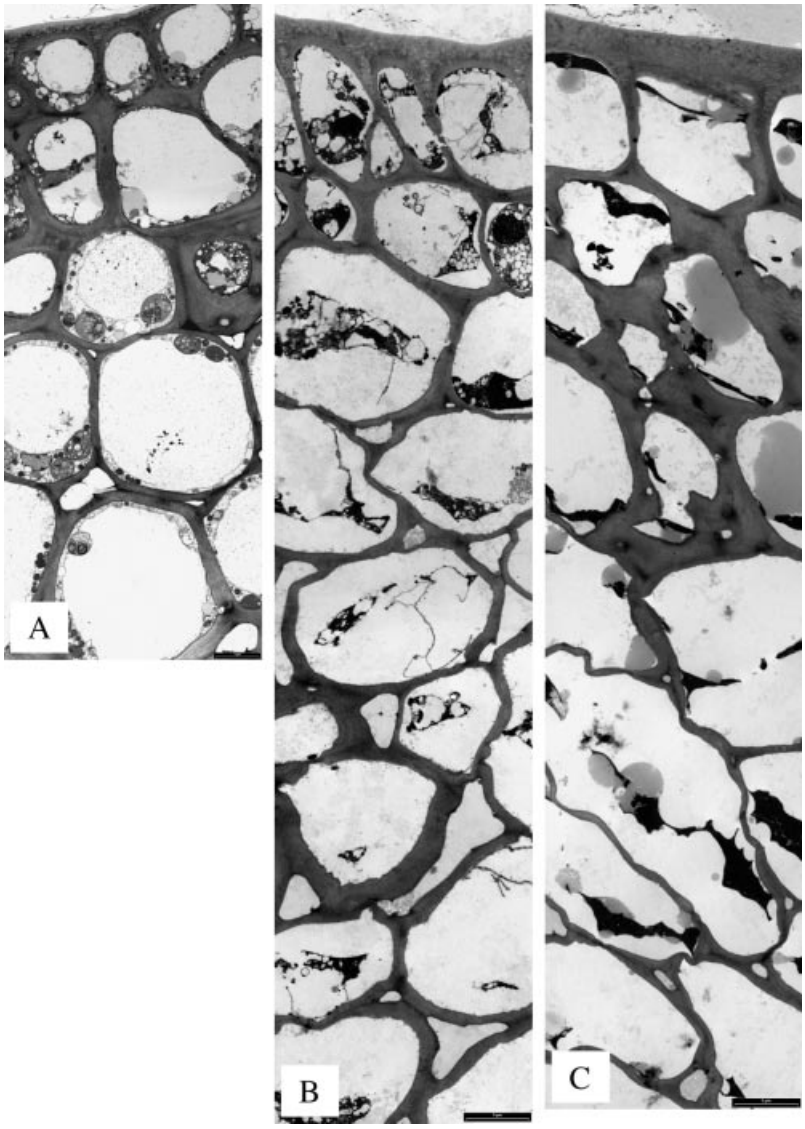

FIG. 6. Oleocellosis development following oil treatment, profile images. A, 30 min, no symptoms. B, 6 h, very slight blemish (collapse = 2, discolouration = 0). C, 10 d, extreme blemish (collapse = 4, discolouration = 5). Bars = 5 µm.

Oil bodies were less evident in lower cell layers, but were positioned close to plasmodesmata (Fig. 7G) and filled intercellular spaces between cortex cells, to a depth of approx. nine cell layers.

By 6 h, very slight external signs of rind collapse had developed; however, the rind profile had changed dramatically, showing various stages of cell content degeneration (Fig. 6B). Portions of the plasmalemma were detached from the cell wall. Some cells contained a collapsed protoplast in which little structure could be identified, whereas others were highly vesiculated and contained discrete but degenerating organelles, such as nuclei and mitochondria. Walls of cortex and hypodermal cells showed a slight loss of integrity, and intercellular spaces appeared to be greater in number and size. By 48 h, collapsed protoplasts were present in all cell layers and greater cell wall thickening and folding was observed, which included epidermal cells.

By 10 d, rind collapse and extreme discolouration had developed. The rind profile showed more advanced cell content degeneration, larger numbers of oil bodies in cells and a greater loss of cell wall integrity (Figs 6C and 7H). Oil-damaged cells were present to a depth of 17 cell layers. Further wall thickening was observed in hypodermal and epidermal layers, and folding in cortex and hypodermal layers (Fig. 7H).

DISCUSSION

This study has shown that ultrastructural changes leading to oleocellosis symptoms commence within 30 min of oil application to the fruit surface. Oleocellosis symptoms following mechanical damage are less severe than those following oil application, in terms of both external blemish and epidermal and hypodermal cell degeneration. It is

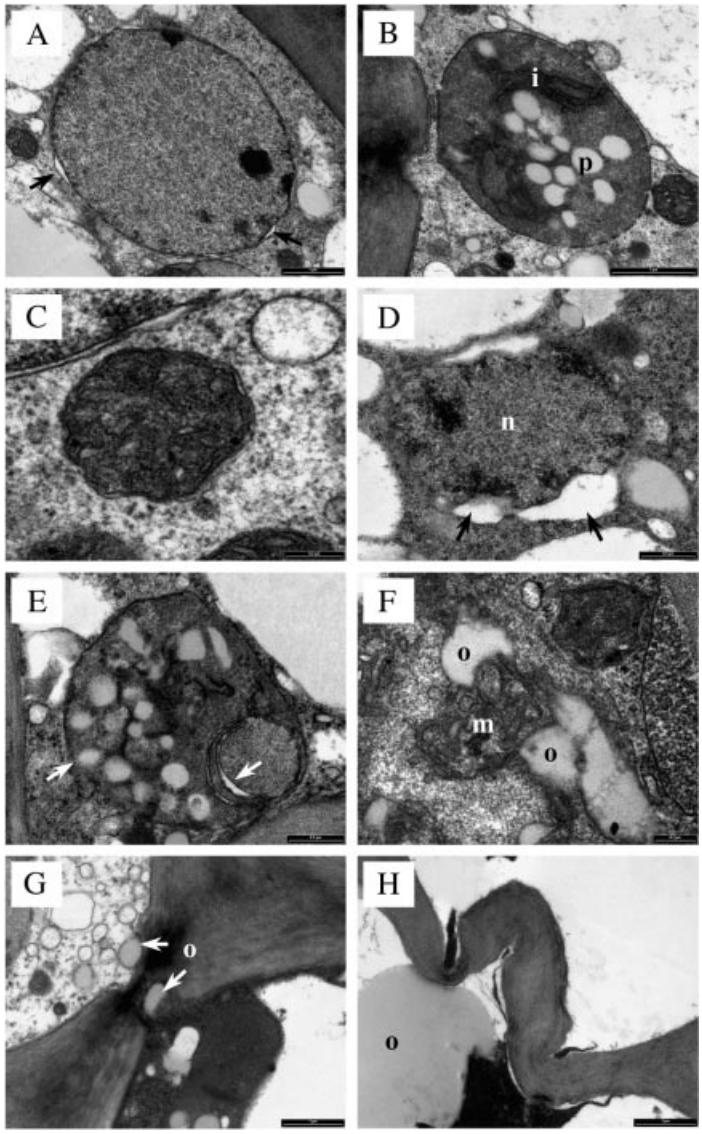

FIG. 7. Untreated (control) and oil-treated tissue, TEM sections. A, Nucleus with an intact envelope and very slight swelling between inner and outer membranes (arrows), in untreated tissue. Bar = 1 μm. B, Plastid (chromoplast) with intact outer membrane, folded inner membrane (i) and lightly stained plastoglobuli (p), in untreated tissue. Bar = 1 μm. C, Mitochondrion with intact double membrane and cristae, in untreated tissue. Bar = 0·2 μm. D, 30 min after oil treatment; nucleus (n) showing significant expansion of the perinuclear space (arrows). Bar = 0·5 μm. E, 30 min after oil treatment; plastid showing signs of outer membrane and internal degeneration (arrows). Bar = 0·5 μm. F, 30 min after oil treatment; mitochondrion (m) with adjacent oil bodies (o). Bar = 0·2 μm. G, 30 min after oil treatment; oil bodies (o) in close association with a plasmodesma. Bar = 1 μm. H, 10 d after oil treatment; wall swelling and folding, in cortex cells containing oil (o). Bar = 1 μm.

proposed that mechanical damage produces openings in the rind that act as a pathway for surface oil movement into the cortex, leading to rapid degeneration of cortical cell contents. In some cases, epidermal and hypodermal cell contents degenerate following mechanical damage, indicating that their cell walls are not always a barrier to oil ingress. In contrast, oil applied to the surface of the rind appears to diffuse through the cuticle and cell wall, causing cell content degeneration of all rind tissues.

Surface oil release was detected following mechanical damage, but no evidence of internal oil release was established. Gland rupture was observed to occur at the junction of the epidermis and the apical region of the gland, or the gland stalk (Knight *et al*., 2001). This confirms previous LM observations of mechanically damaged rind tissue (Labuschagne *et al*., 1977; du Plessis, 1978). Serial sections revealed no other structural disruption to the gland to facilitate oil release into the rind tissue. Observations suggest that the gland stalk is a point of structural weakness and that lateral oil release from the gland directly into the cortical tissue may be prevented by the flattened layers of thick-walled boundary cells that enclose the gland

(Thomson *et al*., 1976). This structural feature is also likely to protect against *in situ* tissue damage by the oil in the absence of mechanical damage.

Previously, separate studies of oleocellosis have reported surface oil release and sub-epidermal rind damage, but a link between the two phenomena has not been identified. Based on our observations, it appears that oil released to the surface may enter the rind via the path of least resistance—through the ruptured gland stalk—into the cortex layers alongside the outer gland wall, and then spread laterally. Gland boundary cell walls appear to be largely impermeable to oil (Thomson *et al*., 1976; Shomer, 1980). Surface oil may, however, enter lower rind layers through other cracks and tears in the rind tissue caused by mechanical damage. This would be similar to the mechanism of water spot described by Scott and Baker (1947), in which water enters the rind via stomata or microscopic cracks formed during tissue expansion. Previously, sub-epidermal cell damage has also been associated with the citrus rind disorders 'preharvest peel pitting' (Medeira *et al*., 1999) and 'rind-oil spot' (Chikaizumi, 2000). In both studies, rind oils were suggested as a possible cause, but underlying mechanisms were not established.

Lipid bodies were in greater abundance in oleocellosis-damaged tissue compared with untreated tissue. Oil was clearly present within cell protoplasts and in intercellular spaces, suggesting both symplastic and apoplastic movement. In mechanically damaged tissue, oil movement may have been aided by the numerous intercellular spaces of the cortex layers. Collenchymatic hypodermal cells had thicker walls than cortex cells, but did not possess suberized or lignified secondary walls that may have restricted oil movement between the two layers. The speed of oil movement in the rind was demonstrated by the presence of oil-filled intercellular spaces to a depth of approx. nine cell layers within 30 min of surface oil application. TEM observations of oil in oleocellosis-damaged tissue were confirmed using confocal microscopy, with degenerated protoplasts observed to take up lipid stain.

Oil-damaged cells appeared to undergo a loss of membrane integrity, followed by degeneration of cell contents. Ultrastructural changes were similar to those observed in oleocellosis of de-greened Shamouti orange fruit (Shomer and Erner, 1989). In that study, advanced protoplast degeneration was observed 3 h after oil treatment. Earlier signs of degeneration were detected in the present study; membrane degeneration was observed as early as 30 min after oil treatment. Oil bodies were also closely associated with misshapen mitochondria and plastids at this time. By 6 h, the degeneration of membranes had induced the destruction of protoplasmic elements, although degenerated nuclei and mitochondria were discernible in some cells. Collapse of the protoplast occurred at approx. 48 h.

Previously, the degenerated contents of an oil-damaged cell have been interpreted as a giant chloroplast (Shomer and Erner, 1989). The giant chloroplast was reported to contain more starch and denser grana than chloroplasts of intact cells. In the present study, TEM observations gave no indication of the preferential fusion of chloroplasts. Vesicular structures in the degenerated protoplast did not show the refractory nature of starch bodies, and material within the degenerated contents was interpreted as strands of disassembled membranes rather than grana. The presence of grana seems unlikely considering that prior to damage, these cells contained chromoplasts, which do not contain a substantial grana system. In addition, speculation by Shomer and Erner (1989) that giant chloroplasts may produce larger amounts of chlorophyll than normal chloroplasts seems unlikely considering the degenerative state of the cells described.

Wall thickening and collapse was observed to take place in oil-damaged cells. The cell wall thickening was most likely to be attributable to swelling. Cell collapse, which appeared to result from folding of the cell walls, was not detected until advanced cell content degeneration had occurred. However, the fact that parenchymatic cortex cells showed signs of collapse before thicker-walled collenchymatic hypodermal cells, suggests that collapse may have resulted from loss of physical strength (Labuschagne *et al*., 1977; du Plessis, 1978; Shomer and Erner, 1989). Flattened cell layers of the oleocellosis-damaged rind have been associated with a change from radial to tangential division, in a process likened to that observed in wounding (B. L. Wild, pers. comm.). In the present study, there was no evidence of dividing cells, and suberin and lignin, which are commonly formed at early stages of the wounding response (Larson, 1994), were not present in oleocellosis-damaged tissues.

Past studies have attributed rind discolouration to changes in the fruit cuticle or epidermis (Labuschagne *et al*., 1977; Sawamura *et al*., 1984; B. L. Wild, pers. comm.). Based on time-sequence observations, it seems likely, however, that surface discolouration is a result of advanced cell content degeneration and cell wall changes, extending a number of layers into the rind. The reduced rind discolouration observed in penetrometer-damaged fruit compared with surface oil-treated fruit may be explained by the fact that upper layers of the flavedo, the coloured portion of the rind, remained intact.

Given the rapid breakdown in cellular compartmentalization, it is also possible that browning reactions involving enzymes such as polyphenol oxidase (PPO) and peroxidase are involved. PPO catalyses the oxidation of phenols that are sequestered in the vacuole (Mayer and Harel, 1979) but released upon tonoplast breakdown, observed at early stages of oleocellosis development. The involvement of PPO is also supported by the fact that oleocellosis-damaged tissues have been reported to show reduced darkening under low oxygen storage conditions (Wild, 1998).

ACKNOWLEDGEMENTS

This work was funded by the Citrus Board of South Australia through an Australian Research Council Australian Postgraduate Award (Industry). We wish to thank Gueue Bros Pty Ltd for their fruit; Lyn Waterhouse, Dr Meredith Wallwork and Linda Olssen for technical

assistance with microscopy; and Michelle Lorimer for statistical advice.

LITERATURE CITED

Brundrett MC, Kendrick B, Peterson CA. 1991. Efficient lipid staining in plant material with Sudan Red 7B or Fluoral Yellow 088 in polyethylene glycol-glycerol. *Biotechnic and Histochemistry* **66**: 111–116.

Cahoon GA, Grover BL, Eaks IL. 1964. Cause and control of oleocellosis on lemons. *Proceedings of the American Society for Horticultural Science* **84**: 188–198.

Chikaizumi S. 2000. Mechanisms of rind-oil spot development in 'Encore' (*Citrus nobilis* Lour. X *C. deliciosa* Ten.) fruit. *Journal of the Japanese Society for Horticultural Science* **69**: 149–155.

du Plessis SF. 1978. Skilprobleme by sitrus: oleoselloseen Gepokte skil. *Citrus and Sub-tropical Fruit Journal* **534**: 12–16.

Eaks IL. 1968. Rind disorders of oranges and lemons in California. In: Chapman HD, ed. *First international citrus symposium.* Riverside, USA: University of California, 1343–1354.

Erner Y. 1982. Reduction of oleocellosis damage in Shamouti orange peel with ethephon preharvest spray. *Journal of Horticultural Science* **57**: 129–133.

Fawcett HS. 1916. A spotting of citrus fruits due to the action of oil liberated from the rind. *California Agricultural Experiment Station Bulletin* **266**: 259–270.

Hughes J, McCully ME. 1975. The use of an optical brightener in the study of plant structure. *Stain Technology* **50**: 319–321.

Jensen WA. 1962. *Botanical histochemistry*. San Francisco: W. H. Freeman and Co.

Knight TG, Klieber A, Sedgley M. 2001. The relationship between oil gland and fruit development in Washington navel orange (*Citrus sinensis* L. Osbeck). *Annals of Botany* **88**: 1039–1047.

Labuschagne JL, Holtzhausen LC, du Plessis SF. 1977. 'N Anatomiese ondersoek na die voorkoms van oleocellosis en gepokte skil by *Citrus sinensis* (L.) Osbeck. *Citrus and Sub-tropical Fruit Journal* **527**: 7–14.

Larson PR. 1994. *The vascular cambium: development and structure*. Berlin: Springer-Verlag.

Levy Y, Greenberg J, Ben-Anat S. 1979. Effect of ethylene-releasing compounds on oleocellosis in 'Washington' navel oranges. *Scientia Horticulturaee* **11**: 61–68.

Loveys B, Tugwell BL, Bevington K, Wild BL. 1998. New approaches to combating oleocellosis. *Horticultural Research and Development Corporation (HRDC) Final Report, Project CT 403*.

Mayer AM, Harel E. 1979. Polyphenol oxidases in plants. *Phytochemistry* **18**: 193–215.

Medeira MC, Maia MI, Vitor RF. 1999. The first stages of pre-harvest 'peel pitting' development in 'Encore' mandarin. An histological and ultrastructural study. *Annals of Botany* **83**: 667–673.

O'Brien TP, McCully ME. 1981. *The study of plant structure. Principles and selected methods*. Melbourne: Termarcarphi Pty Ltd.

Sawamura M, Manabe T, Oonishi S, Yasuoka K, Kusunose H. 1984. Effects of rind oils and their components on the induction of rind spot in citrus species. *Journal of Horticultural Science* **59**: 575–579.

Scott FM, Baker KC. 1947. Anatomy of Washington navel orange rind in relation to water spot. *Botanical Gazette* **108**: 459–475.

Shaw PE. 1979. Review of quantitative analyses of citrus essential oils. *Journal of Agricultural and Food Chemistry* **27**: 246–257.

Shomer I. 1980. Sites of production and accumulation of essential oils in citrus fruits. *Electronic microscopy* **2**: 256–257.

Shomer I, Erner Y. 1989. The nature of oleocellosis in citrus fruits. *Botanical Gazette* **150**: 281–288.

Thomson WW, Platt-Aloia KA, Endress AG. 1976. Ultrastructure of oil gland development in the leaf of *Citrus sinensis* L. *Botanical Gazette* **137**: 330–340.

Whiteside JO, Garnsey SM, Timmer LW. 1988. *Compendium of citrus diseases*. St Paul, Minnesota: APS Press.

Wild BL. 1998. New method for quantitatively assessing susceptibility of citrus fruit to oleocellosis development and some factors that affect its expression. *Australian Journal of Experimental Agriculture* **38**: 279–285.